

Revised Analyses of Postdetection Switched Combining in Nakagami- m Fading

Sasan Haghani, *Student Member, IEEE*, and Norman C. Beaulieu, *Fellow, IEEE*

Abstract—In two recent papers, the performances of dual-branch postdetection switch-and-stay combining (SSC) for noncoherent orthogonal binary frequency-shift keying (BFSK) and noncoherent orthogonal M -ary frequency-shift keying (MFSK) operating in the presence of slow flat fading modeled by Rayleigh, Nakagami- m , and Rician distributions have been analyzed. In this paper, we show that these previous analyses for the Nakagami- m fading model, which are restricted to integer values of m , are incorrect, and we derive the correct bit-error rate (BER) performances of BFSK and MFSK with dual-branch SSC in Nakagami- m fading for all values of m . Optimum switching thresholds that minimize the BER of BFSK and MFSK with postdetection SSC in Nakagami- m fading are obtained. The performance of postdetection SSC is compared with the performance of predetection SSC, and it is shown that postdetection SSC outperforms predetection SSC for all values of signal-to-noise ratio (SNR). We also show that for a given BER, the performance gain of postdetection SSC over predetection SSC has been overestimated by several decibels in SNR in previous publications.

Index Terms—Diversity combining, fading channels, postdetection diversity, switch-and-stay combining (SSC).

I. INTRODUCTION

TWO PAPERS recently published in these TRANSACTIONS [1], [2] have studied the performance of dual-branch postdetection switch-and-stay combining (SSC) for noncoherent orthogonal binary frequency-shift keying (BFSK) and noncoherent orthogonal M -ary frequency-shift keying (MFSK) in Rayleigh, Nakagami- m , and Rician fading channels. These papers are important, in particular, because they quantify the improvement of postdetection SSC over predetection SSC. In this paper, we show that the analyses of [1] and [2] for the Nakagami- m model, which are restricted to integer values of m , are mathematically incorrect, and we derive correct expressions for the bit-error rate (BER) performances of dual-branch postdetection SSC with BFSK and MFSK in Nakagami- m fading channels. Furthermore, we show that the results published in [1] and [2] overestimate the performance gain of postdetection SSC over predetection SSC by several decibels in signal-to-noise ratio (SNR) for a given BER. We also derive

Paper approved by P. Y. Kam, the Editor for Modulation and Detection for Wireless Systems of the IEEE Communications Society. Manuscript received March 13, 2004; revised November 8, 2004 and March 1, 2005. This paper was presented in part at the IEEE 60th Vehicular Technology Conference, Los Angeles, CA, September 2004.

The authors are with the Department of Electrical Computer Engineering, University of Alberta, Edmonton, AB T6G 2V4, Canada (e-mail: haghani@ece.ualberta.ca; beaulieu@ece.ualberta.ca).

Digital Object Identifier 10.1109/TCOMM.2005.855007

optimum switching thresholds that minimize the error-rate performance of BFSK and MFSK with postdetection SSC in Nakagami- m fading.

The remainder of this paper is organized as follows. In Section II, we correct the results published in [1] for the performance of BFSK with postdetection SSC in Nakagami- m fading. We also derive correct optimum switching thresholds which minimize the BER of BFSK with postdetection SSC in Nakagami- m fading. Numerical examples are given, and it is observed that the performance gain of postdetection SSC over predetection SSC is less than previously reported. In Section III, we correct the previous analysis regarding the error-rate performance of MFSK with postdetection SSC in Nakagami- m fading published in [2], and we derive correct optimum switching thresholds in order to minimize the BER performance. Some numerical examples are presented to verify the analyses, and the performance of MFSK with predetection SSC is compared with that of postdetection SSC. Finally, some conclusions are given in Section IV.

II. AVERAGE BER ANALYSIS OF BFSK WITH POSTDETECTION SSC IN A NAKAGAMI- m FADING CHANNEL

The block diagram of a BFSK system with postdetection SSC is given in [1, Fig. 1] and is not repeated here, for the sake of brevity. The operation of the switching mechanism and the considerations involved in choosing an optimum switching threshold are discussed in [1, Sec. III], and a general expression for the average BER of noncoherent BFSK with postdetection SSC is given in [1, Sec. IV]. These details are summarized here for completeness; only material essential for the development in this paper is recalled.

A. Switching Mechanism and Threshold Determination

Let the random variables (RVs) W_1 and W_2 , corresponding to channels one and two, denote the inputs to the channel switch. Also, let $|W_1(n)|$ and $|W_2(n)|$ denote the amplitude of the RVs W_1 and W_2 at time $t_n = nT_b$. Without loss of generality, we assume that the switch is connected to antenna one. Then, $|W_1(n)|$ is compared with a predetermined switching threshold w_{T_1} . If $|W_1(n)| > w_{T_1}$, the switch will remain connected to antenna one for the next T_b seconds, and it is used to make a decision [1]. Otherwise, the switch is connected to antenna two, regardless of $|W_2(n)|$. Similarly, if the switch is connected to antenna two, it will remain connected to antenna two if $|W_2(n)| > w_{T_2}$ and will switch to antenna one otherwise, again regardless of $|W_2(n)|$.

[1]. A mathematical expression for the switching mechanism given in [1, eqs. (1)–(2)] is

$$W(n) = W_i(n) = \text{if} \begin{cases} W(n-1) = W_i(n-1) \text{ and } |W_i(n)| \geq w_{T_i}, & i=1, 2 \\ \text{or} \\ W(n-1) = W_{\bar{i}}(n-1) \text{ and } |W_{\bar{i}}(n)| \leq w_{T_{\bar{i}}}, & i=1, 2 \end{cases} \quad (1)$$

where \bar{i} denotes the two's complement of i . Also, a general expression for the average BER of BFSK with postdetection SSC is given in [1, Sec. IV]. For the case of independent and identically distributed (i.i.d.) branches, the average BER can be written as

$$P_b(E) = F_W(-w_T) + [F_W(w_T) - F_W(-w_T)]F_W(0) \quad (2)$$

where $F_W(\cdot)$ denotes the cumulative distribution function (CDF) of the RV W .

B. Analysis

In [1, p. 1598], the authors have assumed that for Nakagami- m fading and integer values of m , the RV W_{11} , shown in [1, Fig. 1], has a central chi-squared distribution. In the following, we show that this is indeed incorrect, and we find the correct distribution of W_{11} for integer as well as noninteger values of m . Then, we derive the correct BER of BFSK with dual-branch postdetection SSC using the BER expression given in [1, Sec. IV].

Without loss of generality, we assume that the binary symbol corresponding to f_1 is transmitted, and the switch is connected to antenna one. Then the decision variable W_1 can be written as [1, eq. (15)]

$$W_1 = W_{11} - W_{12} = |2E_b\alpha_1 e^{j\theta_1} + N_{11}|^2 - |N_{12}|^2 \quad (3)$$

where E_b is energy per transmitted bit, N_{11} and N_{12} are zero-mean complex Gaussian RVs with variance $4E_bN_0$, and $\alpha_1 e^{j\theta_1}$ is the complex gain of channel one, where α_1 is the amplitude and θ_1 is the phase.

To obtain the CDF of W_{11} we first derive the CDF of W_{11} under static conditions. i.e., we first derive the CDF of W_{11} , assuming α_1 and θ_1 are fixed, and then we average the CDF of W_{11} over the joint probability density function (pdf) of α_1 and θ_1 . To begin, we note that the RV W_{11} can be written as

$$\begin{aligned} W_{11} &= |2E_b\alpha_1 e^{j\theta_1} + N_{11}|^2 \\ &= |2E_b\alpha_1 + e^{-j\theta_1} N_{11}|^2 |e^{j\theta_1}|^2 \\ &= |2E_b\alpha_1 + N_1|^2 \\ &= |2E_b\alpha_1 + N_1^I|^2 + |N_1^Q|^2 \end{aligned} \quad (4)$$

where $N_1 = e^{j\theta_1} N_{11}$, and the fixed phase term $e^{j\theta_1}$ is absorbed in the noise term N_{11} , without changing its statistics [3, p. 292], to yield N_1 . Under the static channel condition, W_{11} is a non-central chi-squared RV with two degrees of freedom (DOFs), and its CDF is given by

$$F_{W_{11}|\alpha_1, \theta_1}(w) = 1 - Q_1\left(\frac{2E_b\alpha_1}{\sigma}, \frac{\sqrt{w}}{\sigma}\right) \quad (5)$$

where $\sigma^2 = 2E_bN_0$ and $Q_1(a, b)$ is the first-order Marcum Q-function, and is defined as [4, eq. (4.11)]

$$Q_1(a, b) = \int_b^\infty x \exp\left(-\frac{x^2 + a^2}{2}\right) I_0(ax) dx \quad (6)$$

and where $I_0(x)$ is the zeroth-order modified Bessel function of the first kind [5, Sec. 8.43].

To obtain the unconditional CDF of W_{11} , we average $F_{W_{11}|\alpha_1, \theta_1}(w)$ over the joint pdf of (α_1, θ_1) to get

$$\begin{aligned} F_{W_{11}}(w) &= \int_{\alpha_1=0}^\infty \int_{\theta_1=0}^{2\pi} F_{W_{11}|\alpha_1, \theta_1}(w) f(\alpha_1, \theta_1) d\alpha_1 d\theta_1 \quad (7a) \\ &= \int_{\alpha_1=0}^\infty \left(1 - Q_1\left(\frac{2E_b\alpha_1}{\sigma}, \frac{\sqrt{w}}{\sigma}\right)\right) \\ &\quad \times \left\{ \int_{\theta_1=0}^{2\pi} f(\alpha_1, \theta_1) d\theta_1 \right\} d\alpha_1 \quad (7b) \\ &= \int_{\alpha_1=0}^\infty \left(1 - Q_1\left(\frac{2E_b\alpha_1}{\sigma}, \frac{\sqrt{w}}{\sigma}\right)\right) f(\alpha_1) d\alpha_1. \end{aligned} \quad (7c)$$

Under the Nakagami- m assumption, the marginal pdf of α_1 is given by [4, eq. (2.20)]

$$p_{\alpha_1}(\alpha_1) = \frac{2\alpha_1^{2m_1-1}}{\Gamma(m_1)} \left(\frac{m_1}{\Omega_1}\right)^{m_1} \exp\left(-\frac{m_1\alpha_1^2}{\Omega_1}\right) \quad (8)$$

where m_1 is the fading parameter corresponding to channel one, $\Omega_1 = \mathbb{E}(\alpha_1^2)$, and $\mathbb{E}(\cdot)$ denotes the expectation operation.

To proceed, we first define $\gamma_1 = \alpha_1^2 E_b / N_0$ and $\bar{\gamma}_1 = \Omega_1 E_b / N_0$ as the instantaneous SNR and the average SNR on the first branch, respectively. Then, substituting (8) in (7c) and making the change of variable $\alpha_1^2 = \gamma_1 N_0 / E_b$, we obtain

$$\begin{aligned} F_{W_{11}}(w) &= \int_0^\infty \left(1 - Q_1\left(\sqrt{2\gamma_1}, \frac{\sqrt{w}}{\sigma}\right)\right) \\ &\quad \times \left(\frac{m_1}{\bar{\gamma}_1}\right)^{m_1} \frac{\gamma_1^{m_1-1}}{\Gamma(m_1)} \exp\left(-\frac{m_1\gamma_1}{\bar{\gamma}_1}\right) d\gamma_1. \end{aligned} \quad (9)$$

To calculate the integral in (9), we replace the Bessel function by its series expansion [1, eq. (8.445)]. The result, after some integral evaluations, is

$$\begin{aligned} F_{W_{11}}(w) &= 1 - C_1(m_1, \bar{\gamma}_1) \exp\left(-\frac{w}{2\sigma^2}\right) \\ &\quad \times \sum_{k=0}^\infty C_2(k, m_1, \bar{\gamma}_1) \sum_{n=0}^k \frac{w^n}{(2\sigma^2)^n n!} \end{aligned} \quad (10a)$$

where $C_1(m, \bar{\gamma})$ and $C_2(k, m, \bar{\gamma})$ are defined as

$$C_1(m, \bar{\gamma}) = \frac{\left(\frac{m}{\bar{\gamma}}\right)^m}{\Gamma(m) \left(1 + \frac{m}{\bar{\gamma}}\right)^m} \quad (10b)$$

$$C_2(k, m, \bar{\gamma}) = \frac{\Gamma(m+k)}{k! \left(1 + \frac{m}{\bar{\gamma}}\right)^k}. \quad (10c)$$

The pdf of W_{11} can now be obtained from its CDF as

$$f_{W_{11}}(w) = \frac{C_1(m_1, \bar{\gamma}_1) e^{-(w/2\sigma^2)}}{2\sigma^2} \sum_{k=0}^\infty \frac{C_2(k, m_1, \bar{\gamma}_1) w^k}{k! (2\sigma^2)^k}. \quad (11)$$

Equation (11) clearly shows that the pdf of W_{11} is not central chi-squared.

The RV W_{12} is central chi-square with two DOFs and parameter $2E_b N_0$. Hence, its pdf is given by

$$f_{W_{12}}(w) = \frac{1}{2\sigma^2} \exp\left(-\frac{w}{2\sigma^2}\right). \quad (12)$$

We now proceed to calculate the CDF of W_1 defined in (3). Note that $W_{11} \geq 0$ and $W_{12} > 0$. Therefore, W_1 can be positive or negative. For $W_1 > 0$, using [6, p. 185], the CDF of W_1 can be written as

$$F_{W_1}(w) = \int_0^\infty [F_{W_{11}}(w_2 + w) - F_{W_{11}}(0)] f_{W_{12}}(w_2) dw_2, \quad w > 0. \quad (13a)$$

Substituting (10) and (12) in (13a), using [5, eq. (3.382.4)] and [5, eq. (8.352.2)], and after some mathematical manipulations, we obtain

$$F_{W_1}(w) = 1 - C_1(m_1, \bar{\gamma}_1) e^{-(w/2\sigma^2)} \times \sum_{k=0}^{\infty} \sum_{n=0}^k \sum_{t=0}^n \frac{C_2(k, m_1, \bar{\gamma}_1)}{2^{n+t+1} t!} \left(\frac{w}{\sigma^2}\right)^t, \quad w > 0. \quad (14)$$

For $W_1 < 0$, using [6, p. 186], the CDF of W_1 becomes

$$F_{W_1}(w) = \int_{-w}^\infty [F_{W_{11}}(w_2 + w) - F_{W_{11}}(0)] f_{W_{12}}(w_2) dw_2, \quad w < 0. \quad (15a)$$

Substituting (10) and (12) in (15a), and after some mathematical simplifications, we derive $F_{W_1}(w)$ for $w < 0$ as

$$F_{W_1}(w) = e^{(w/2\sigma^2)} \left[1 - C_1(m_1, \bar{\gamma}_1) \sum_{k=0}^{\infty} \frac{C_2(k, m_1, \bar{\gamma}_1)(2^{k+1} - 1)}{2^{k+1}} \right], \quad w < 0. \quad (16)$$

Similarly, we can obtain the CDF of W_2 , if the switch is connected to antenna 2. Therefore, combining (14) and (16), the CDF of W_1 and W_2 can be written as shown in (17) at the bottom of the page, which corrects [1, eq. (41)] and [1, eq. (42)].

A general expression for the BER of noncoherent BFSK with dual-branch postdetection SSC can now be obtained by substituting (17) in the BER expression given in [1, Sec. IV]. In the case of i.i.d. branches, the BER becomes

$$P_b(E) = \left[1 - C_1(m, \bar{\gamma}) \sum_{k=0}^{\infty} \frac{C_2(k, m, \bar{\gamma})(2^{k+1} - 1)}{2^{k+1}} \right] \times \left[1 - C_1(m, \bar{\gamma}) e^{-(\eta_T \bar{\gamma}/4)} \sum_{k=0}^{\infty} C_2(k, m, \bar{\gamma}) \times \left\{ \sum_{n=0}^k \sum_{t=0}^n \frac{(\eta_T \bar{\gamma})^t}{2^{n+t+1} t!} - \frac{(2^{k+1} - 1)}{2^{k+1}} \right\} \right] \quad (18)$$

where $\eta_T = (w_T/E_b^2 \Omega)$ is the normalized switching threshold. Equation (18) corrects the BER expression given previously [2, eq. (43)] for i.i.d Nakagami- m fading. Note that for numerical calculations, we have used enough terms in the infinite summation in (18) to obtain three significant digits figure accuracy. Note that as the SNR increases, more terms are needed to accurately compute the BER. Our calculations show that typically fewer than 1000 terms are needed to obtain the desired accuracy, even for large values of SNR.

As a check on our results, it is highly desirable to show that (18) reduces to the correct result given in [1, eq. (20)] for the case of Rayleigh fading. Using the identities

$$\sum_{k=0}^{\infty} \left(\frac{y}{1+y}\right)^k \left(\frac{2^{k+1} - 1}{2^{k+1}}\right) = \frac{(1+y)^2}{2+y} \quad (19)$$

and

$$\sum_{k=0}^{\infty} \left(\frac{y}{1+y}\right)^k \sum_{n=0}^k \sum_{t=0}^n \frac{(xy)^t}{2^{n+t+1} t!} = \frac{(1+y)^2}{2+y} \exp\left(\frac{xy^2}{4(1+y)}\right) \quad (20)$$

and after some mathematical simplification, we obtain

$$P_b(E) = \frac{1}{\bar{\gamma} + 2} \left(1 + \frac{1 + \bar{\gamma}}{2 + \bar{\gamma}} \times \left[\exp\left(-\frac{\eta_T \bar{\gamma}}{4}\right) - \exp\left(-\frac{\eta_T \bar{\gamma}}{4(1 + \bar{\gamma})}\right) \right] \right) \quad (21)$$

which is equal to [1, eq. (20)], as expected. The proofs of (19) and (20) are given in Appendix A.

C. Numerical Examples

To further assess the validity of our theoretical results, we have done Monte Carlo simulations. For example, Fig. 1 shows the BER performance of postdetection SSC over i.i.d. Nakagami- m fading for $m = 0.75, 1, 1.5, 2$. Fig. 1 clearly shows that there is excellent agreement between the simulation results and the theoretical results obtained from (18).

Fig. 2 shows the BER performance of noncoherent BFSK with postdetection SSC over i.i.d. Nakagami- m fading for $m =$

$$F_{W_i}(w) = \begin{cases} 1 - C_1(m_i, \bar{\gamma}_i) e^{-(w/2\sigma^2)} \sum_{k=0}^{\infty} \sum_{n=0}^k \sum_{t=0}^n \frac{C_2(k, m_i, \bar{\gamma}_i)}{2^{n+t+1} t!} \left(\frac{w}{\sigma^2}\right)^t, & w > 0 \\ e^{(w/2\sigma^2)} \left[1 - C_1(m_i, \bar{\gamma}_i) \sum_{k=0}^{\infty} \frac{C_2(k, m_i, \bar{\gamma}_i)(2^{k+1} - 1)}{2^{k+1}} \right], & w < 0, \quad i = 1, 2 \end{cases} \quad (17)$$

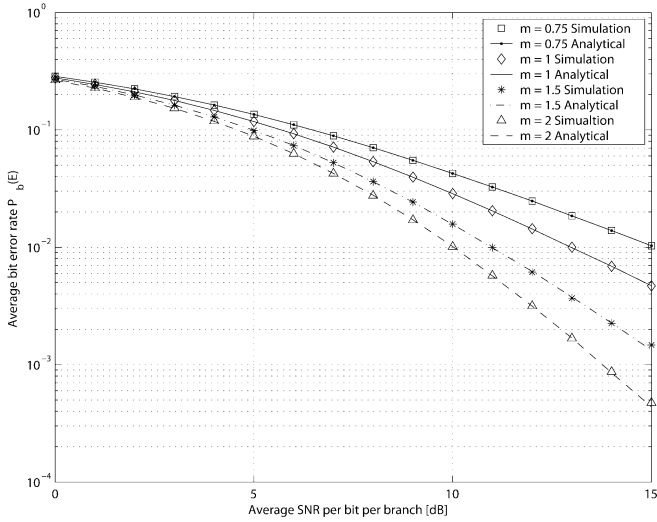


Fig. 1. Average BER of noncoherent BFSK with postdetection SSC versus SNR for $m = .75, 1, 1.5, 2$.

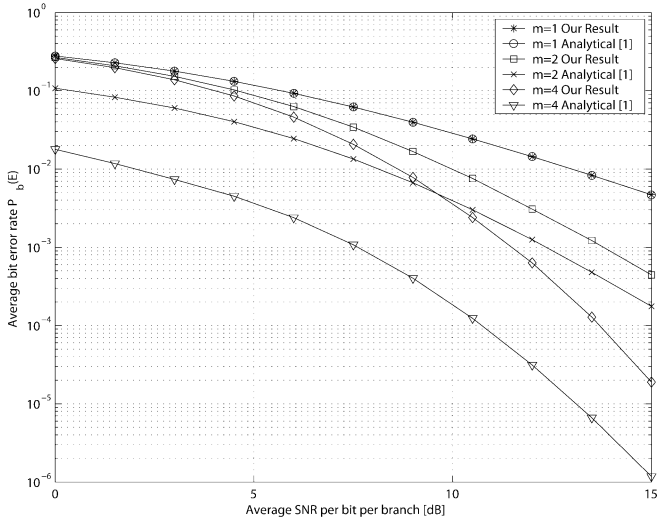


Fig. 2. Average BER of noncoherent BFSK with postdetection SSC versus SNR for $m = 1, 2, 4$.

1, 2, 4, obtained theoretically using (18), and also from simulation together with the analytical results given in [1], also for $m = 1, 2, 4$. We point out that no simulation results were presented in [1]. Fig. 2 clearly shows that the results of [1] are only correct for $m = 1$, which corresponds to Rayleigh fading. For other values of m , the results of [1] overestimate the performance of the system by several decibels in SNR. For example, for $m = 2$ and at a BER of 10^{-2} , the SNR difference between the correct result and the incorrect result is 1.842 dB. For $m = 4$ and at a BER of 10^{-4} , the SNR difference between the correct result and the incorrect result is 3.318 dB. It is important to note that to obtain the results of Figs. 1 and 2, the optimal switching threshold is calculated for each value of SNR numerically.

Figs. 3–5 show the average BER of noncoherent BFSK with postdetection SSC versus the normalized switching threshold for i.i.d. Nakagami- m fading with $m = .75, 2, 4$ for several values of average SNR. These figures show that an optimum threshold exists for every SNR value, and that the optimum threshold decreases as the average SNR increases. For each SNR

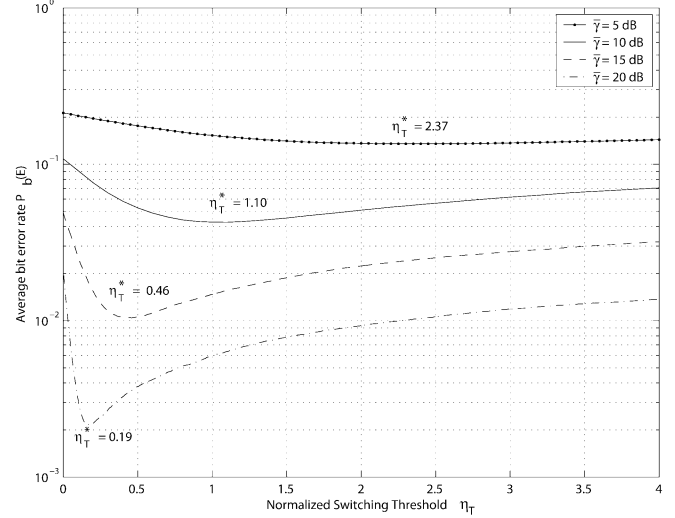


Fig. 3. Average BER of noncoherent BFSK over i.i.d. Nakagami- m fading channels with postdetection SSC versus the normalized switching threshold with $m = 0.75$.

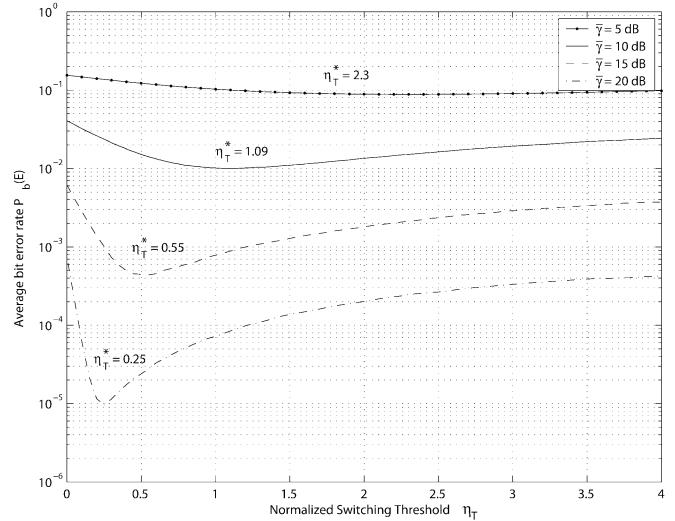


Fig. 4. Average BER of noncoherent BFSK with postdetection SSC versus the normalized switching threshold over i.i.d. Nakagami- m fading channels with $m = 2$.

value, the optimum threshold is indicated in the figures. For example, Fig. 3 shows that for $m = 0.75$, the optimum normalized threshold for $\bar{\gamma} = 5, 10, 15, 20$ dB is 2.37, 1.10, 0.46, and 0.18, respectively. Figs. 4 and 5 correct [1, Fig. 9].

Figs. 3–5 show that an optimal value for the switching threshold exists. This optimal value can be obtained by solving

$$\left. \frac{dP_b(E)}{d\eta_T} \right|_{\eta_T = \eta_T^*} = 0. \quad (22)$$

Substituting (18) in (22), and after some mathematical manipulation, one obtains

$$\begin{aligned} & -\frac{\bar{\gamma}}{4} \exp\left(-\frac{\bar{\gamma}\eta_T}{4}\right) \sum_{k=0}^{\infty} \frac{C_2(k, m, \bar{\gamma})(2^{k+1} - 1)}{2^{k+1}} \\ & -\frac{\bar{\gamma}}{4} \exp\left(\frac{\bar{\gamma}\eta_T}{4}\right) \sum_{k=0}^{\infty} \sum_{n=0}^k \frac{\Gamma\left(\frac{n+1, \bar{\gamma}\eta_T}{2}\right)}{n!2^{n+1}} \\ & +\frac{\bar{\gamma}}{2} \exp\left(-\frac{\bar{\gamma}\eta_T}{4}\right) \sum_{k=0}^{\infty} \sum_{n=0}^k \frac{(\bar{\gamma}\eta_T)^n}{n!2^{2n+1}} = 0. \end{aligned} \quad (23)$$

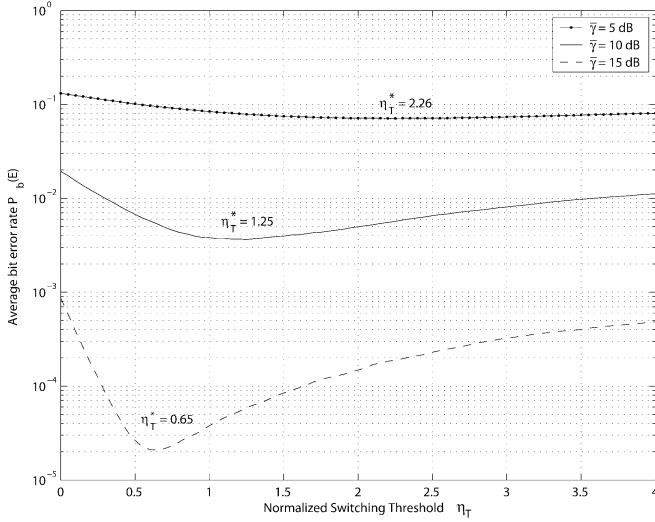


Fig. 5. Average BER of noncoherent BFSK over i.i.d. Nakagami- m fading channels with postdetection SSC versus the normalized switching threshold with $m = 4$.

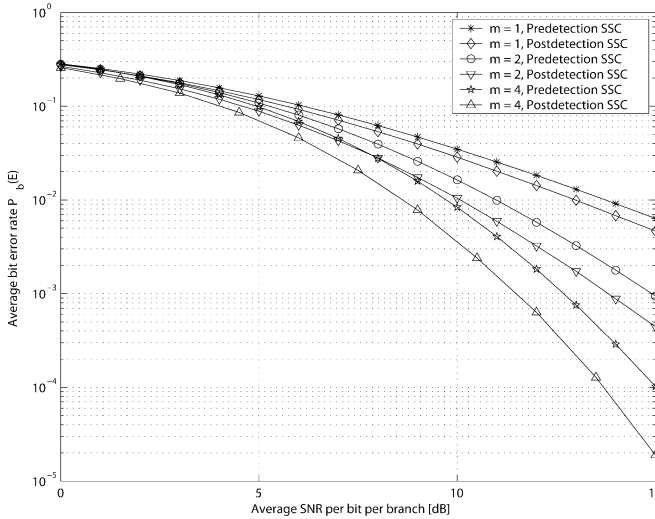


Fig. 6. Comparison of the average BER of noncoherent BFSK in i.i.d. Nakagami- m fading with predetection and postdetection SSC for $m = 1$ and $m = 2$.

The root of (23) is the optimum switching threshold. Equation (23) is given to correct [1, eq. (45)]. However, in practice, it is easier and quicker to obtain the optimum switching threshold by using a simple step search.

Fig. 6 compares the optimal average BERs of noncoherent BFSK with predetection and postdetection SSC for Nakagami- m channels with $m = 1, 2, 4$. Fig. 6 shows that as the SNR increases, the gain of postdetection SSC increases over the gain of predetection SSC. Furthermore, for a given BER, the SNR difference in performance between predetection SSC and postdetection SSC increases as the fading parameter m increases. For example, at a BER of 10^{-2} and for $m = 2$, the SNR difference between predetection and postdetection SSC is 0.8 dB, while at the same SNR and for $m = 4$, the SNR difference between predetection SSC and postdetection SSC is 1.1 dB. This is expected, since increasing the m parameter results in a better channel, as does increasing the SNR.

Fig. 6 also shows that at a given BER, the SNR difference between predetection and postdetection SSC is less than the SNR difference reported in [1, Fig. 10]. For example, at a BER of 10^{-3} and $m = 2$, the SNR difference between predetection and postdetection SSC, as shown in Fig. 6, is only 1.1 dB, whereas in [1, Fig. 10], the SNR difference is 2.0 dB.

III. AVERAGE SER ANALYSIS OF MFSK WITH POSTDETECTION SSC IN A NAKAGAMI- m FADING CHANNEL

A. Analysis

A block diagram of an MFSK system with dual-branch postdetection SSC is shown in [2, Fig. 1], and is not repeated here for the sake of brevity. The switching mechanism is the same as that explained in Section II-A. A general expression for the average symbol-error rate (SER) of noncoherent MFSK with dual-branch SSC is given in [2, eq. (8)]. From [2, eq. (8)], one can see that to calculate the SER, one needs to obtain the pdfs and CDFs of W_{ij} , $i = 1, 2$, $j = 1, \dots, M$, as shown in [2, Fig. 1] and defined as [2]

$$W_{11} = |2E_s\alpha_1 e^{j\theta_1} + N_{11}|^2 \quad (24)$$

$$W_{21} = |2E_s\alpha_2 e^{j\theta_2} + N_{21}|^2 \quad (25)$$

$$W_{jm} = |N_{jm}|^2, \quad j = 1, 2, \quad m = 2, \dots, M \quad (26)$$

where $\alpha_i e^{j\theta_i}$, $i = 1, 2$ are the complex gains of the channel, and N_{ij} , $i = 1, 2$, $j = 1, \dots, M$ are zero mean, complex Gaussian RVs with variance $4E_b N_0$.

In [2], the authors have mistakenly assumed that the RVs W_{11} and W_{21} are central chi-squared. Using similar analyses to that in the previous section, one can derive the pdfs and CDFs of the RVs defined in (24)–(26). Then substituting these pdfs and CDFs in [2, eq. (8)], one obtains the average SER of MFSK with postdetection SSC in Nakagami- m fading for arbitrary values of m . In the case of i.i.d. Nakagami- m fading, after many mathematical simplifications, we obtain a simplified expression for the SER as

$$\begin{aligned} P_s(E) &= 1 - C_1(m, \bar{\gamma}) \sum_{k=0}^{\infty} \sum_{l=0}^{M-1} (-1)^l \binom{M-1}{l} \\ &\quad \times \frac{C_2(k, m, \bar{\gamma})}{k!(l+1)^{k+1}} \Gamma\left(k+1, \frac{(1+l)\bar{\gamma}\eta_T}{4}\right) \\ &\quad - \left\{ 1 - C_1(m, \bar{\gamma}) e^{-(\bar{\gamma}\eta_T/4)} \sum_{k=0}^{\infty} C_2(k, m, \bar{\gamma}) \right. \\ &\quad \quad \left. \times \sum_{n=0}^k \frac{(\bar{\gamma}\eta_T)^n}{4^n n!} \right\} \left(1 - e^{-(\bar{\gamma}\eta_T/4)} \right)^{M-1} \\ &\quad \times C_1(m, \bar{\gamma}) \sum_{k=0}^{\infty} \sum_{l=0}^{M-1} (-1)^l \binom{M-1}{l} \\ &\quad \times \frac{C_2(k, m, \bar{\gamma})}{(l+1)^{k+1}} \end{aligned} \quad (27)$$

where $\eta_T = (w_T/\Omega E_s^2)$ is the normalized switching threshold. Similar to the BFSK case, our calculations indicate that, typically, fewer than 1000 terms are needed to obtain the desired accuracy, even for large values of SNR. Note that (27) corrects

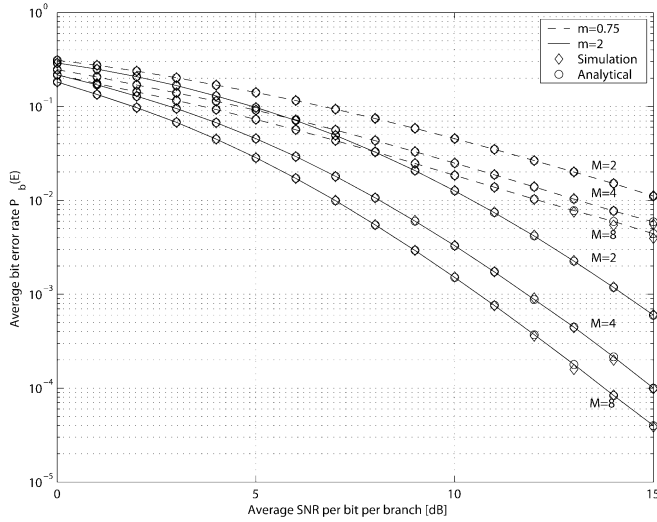


Fig. 7. Average BER of noncoherent MFSK as a function of average SNR per bit per branch over i.i.d. Nakagami- m fading channels with postdetection SSC for $M = 2, 4, 8$ and for $m = 0.75, 2$.

[2, eq. (36)] for i.i.d. Nakagami- m fading. Note that for orthogonal MFSK, the BER can be related to the SER by $P_b(E) = (M/(2(M-1)))P_s(E)$ [3].

For $m = 1$, which corresponds to i.i.d. Rayleigh fading, it is shown in Appendix B that (27) reduces to

$$\begin{aligned}
 P_s(E) &= 1 - \sum_{l=0}^{M-1} \binom{M-1}{l} \frac{(-1)^l}{1+l(1+\bar{\gamma})} \\
 &\quad \times \exp\left(-\frac{\eta_T \bar{\gamma}(1+l(1+\bar{\gamma}))}{4(1+\bar{\gamma})}\right) \\
 &\quad - \left[1 - \exp\left(-\frac{\bar{\gamma}\eta_T}{4(1+\bar{\gamma})}\right)\right] \\
 &\quad \times \left[1 - \exp\left(-\frac{\eta_T \bar{\gamma}}{4}\right)\right]^{M-1} \\
 &\quad \times \sum_{l=0}^{M-1} \binom{M-1}{l} \frac{(-1)^l}{1+l(1+\bar{\gamma})} \quad (28)
 \end{aligned}$$

which is equal to [2, eq. (16)], as expected.

B. Numerical Examples

Fig. 7 shows the BER performance of MFSK with postdetection SSC for $M = 2, 4, 8$ over i.i.d. Nakagami- m fading, with $m = 0.75, 2$ as a function of SNR per branch per bit, obtained from simulation and the theoretical results given in (27). Fig. 7 confirms the validity of our results. Note that the results of Fig. 7 are obtained by calculating the optimal threshold value for each value of SNR.

A figure similar to Fig. 2, comparing the results obtained in (27) and [2, eq. (36)], could not be produced simply because the theoretical expression given in [2, eq. (36)] gives values that are outside plots having any reasonable axes scales.

Figs. 8 and 9 show the average SER of noncoherent 4-ary FSK over i.i.d. Nakagami- m fading channels with postdetection SSC as a function of the normalized switching threshold

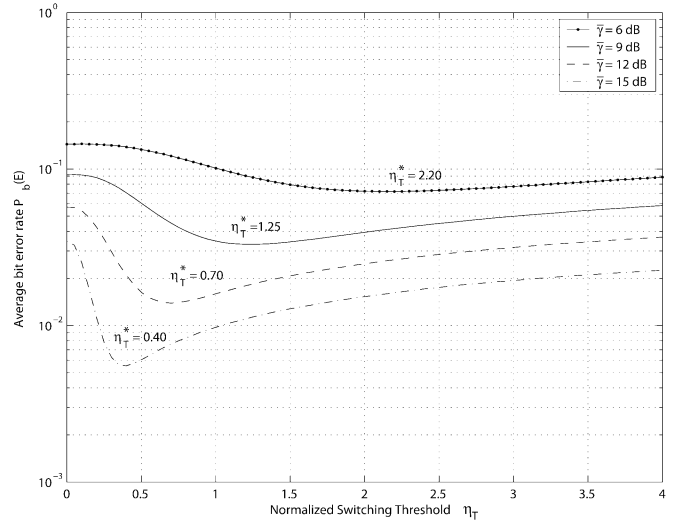


Fig. 8. Average SER of noncoherent QFSK over i.i.d. Nakagami- m fading channels with postdetection SSC versus the normalized switching threshold with $m = 0.75$.

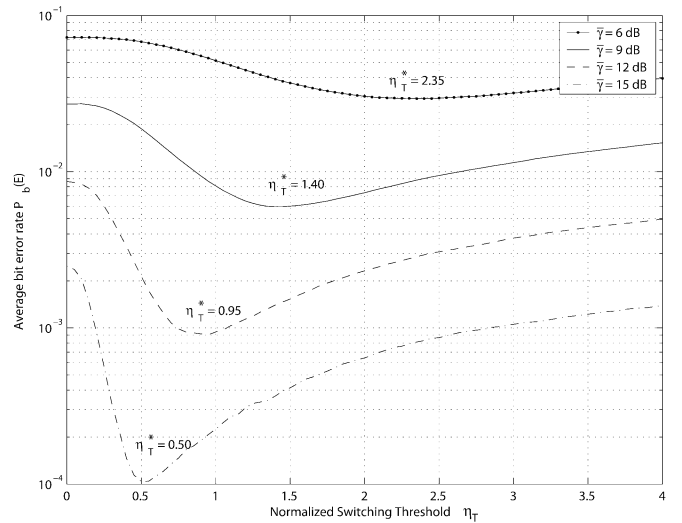


Fig. 9. Average SER of noncoherent QFSK over i.i.d. Nakagami- m fading channels with postdetection SSC versus the normalized switching threshold with $m = 2$.

for $m = 0.75, 2$ and for several values of SNR, respectively. For each value of SNR, the optimum switching threshold is reported on the figures. Figs. 8 and 9 show that an optimum threshold exists for each value of SNR. Similar to [2, Fig. 1], which is obtained for i.i.d. Rayleigh fading, the optimal switching threshold is a decreasing function of the average SNR. This implies that when the SNR is larger, the system will switch more often to exploit better fading conditions on the other channel [2]. Figs. 8 and 9 also show that for each value of SNR, as the fading parameter m increases, the optimal threshold value increases. For example, at an average SNR of 15 dB and for $m = 0.75, 2$, the optimal switching threshold is 0.38 and 0.55, respectively. Thus, the system will switch less frequently when operating in lightly faded channels than when operating in severely faded channels. Figs. 8 and 9 clearly show that for each value of SNR, an optimal

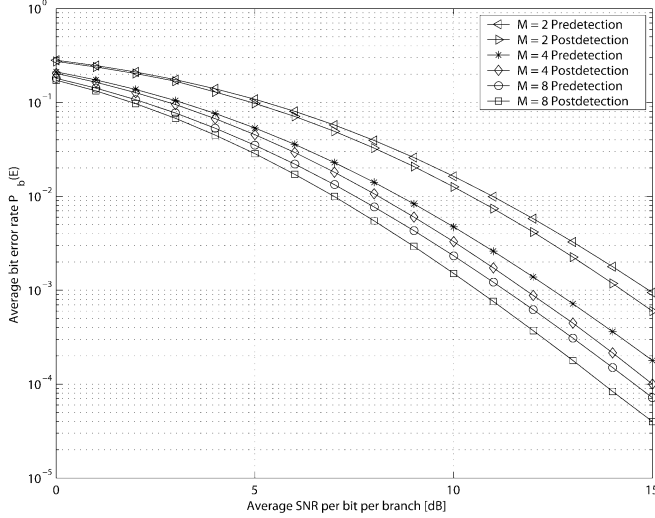


Fig. 10. Average BER of noncoherent MFSK as a function of average SNR per bit per branch with predetection and postdetection SSC for $M = 2, 4, 8$. The branch fading is i.i.d. Nakagami with $m = 2$.

value for the switching threshold exists. The optimal threshold value η_T^* can be obtained by solving

$$\left. \frac{dP_s(E)}{d\eta_T} \right|_{\eta_T=\eta_T^*} = 0. \quad (29)$$

Substituting (27) in (29), one can obtain an expression whose solution is the optimum threshold value, and which corrects the transcendental equation given in [2, eq. (45)]. Note that similar to the case for BFSK, we found it easier for practical purposes to obtain this switching threshold using a simple step search.

It is important to compare the performance of postdetection and predetection SSC combining in fading channels. For predetection SSC, an analytical expression for the SER performance of MFSK with predetection SSC is given in [2]. Using this expression and (27), the average BER of noncoherent MFSK with predetection and postdetection SSC is plotted in Fig. 10 for $M = 2, 4, 8$ as a function of the average SNR per bit per branch, with fading parameter $m = 2$. In Fig. 10, the optimum switching threshold is obtained for each value of SNR for both predetection and postdetection SSC combining. As expected, postdetection SSC outperforms predetection SSC for all values of SNR. Also, Fig. 10 shows that the performance difference between predetection and postdetection SSC increases slightly as M increases. For example, at a BER of 10^{-3} the SNR difference between predetection SSC and postdetection SSC is 0.6 and 0.7 dB for $M = 2$ and $M = 8$, respectively.

IV. CONCLUSION

In this paper, we have corrected previous results published on the performances of BFSK and MFSK with dual-branch postdetection SSC combining in Nakagami- m fading channels. Optimum switching thresholds for minimizing the BER of BFSK and MFSK with postdetection SSC have been derived. We have also compared the performances of BFSK and MFSK with predetection and postdetection SSC in Nakagami- m fading channels. It was observed that postdetection SSC outperforms predetection SSC for all values of SNR, though the performance differences are less than previously reported.

APPENDIX A

In this appendix, we prove (19) and (20). To prove (19), we make the change of variables $z = (y/(1+y))$ in (19), yielding

$$\sum_{k=0}^{\infty} \left(\frac{2^{k+1} - 1}{2^{k+1}} \right) z^k = \frac{1}{(2-z)(1-z)}. \quad (30)$$

One can now show that the left of (30) is the Taylor series for the right of (30) using standard techniques, and hence, the proof is complete.

To prove (20), we write the right side of (20) as

$$\begin{aligned} \frac{(1+y)^2}{2+y} \exp\left(\frac{xy^2}{4(1+y)}\right) &= \sum_{k=0}^{\infty} \left(\frac{y}{1+y}\right)^k \left(\frac{2^{k+1}-1}{2^{k+1}}\right) \\ &\times \sum_{k=0}^{\infty} \left(\frac{y}{1+y}\right)^k \frac{(xy)^k}{k!4^k} \end{aligned} \quad (31)$$

where we have used (19), and the exponential term is replaced by its Taylor series expanded in terms of x . Next, we use [5, eq. (0.316)] to write (31) as

$$\sum_{k=0}^{\infty} \left(\frac{y}{1+y}\right)^k \sum_{n=0}^k \frac{(2^{k-n+1}-1)(xy)^k}{n!2^{n+k+1}}. \quad (32)$$

Now, comparing (32) and the left of (20), one only needs to show that

$$\sum_{n=0}^k \frac{(2^{k-n+1}-1)(xy)^k}{n!2^{n+k+1}} = \sum_{n=0}^k \sum_{t=0}^n \frac{(xy)^t}{2^{n+t+1}t!} \quad (33)$$

which can be proved using a routine mathematical induction. Hence, the proof is complete.

APPENDIX B

In this appendix, we prove that for $m = 1$, (27) reduces to (28). To verify this, it is sufficient to show that

$$\frac{\bar{\gamma} + 1}{1 + l(1 + \bar{\gamma})} = \sum_{k=0}^{\infty} \frac{\left(\frac{\bar{\gamma}}{1+\bar{\gamma}}\right)^k}{(l+1)^{k+1}} \quad (34)$$

and

$$\begin{aligned} \frac{1}{1+\bar{\gamma}} e^{-(\bar{\gamma}\eta_T/4)} \sum_{k=0}^{\infty} \left(\frac{\bar{\gamma}}{1+\bar{\gamma}}\right)^k \sum_{n=0}^k \frac{(\bar{\gamma}\eta_T)^n}{4^n n!} \\ = \exp\left(-\frac{\bar{\gamma}\eta_T}{4(1+\bar{\gamma})}\right) \end{aligned} \quad (35)$$

and

$$\begin{aligned} \frac{1}{1+\bar{\gamma}} \sum_{k=0}^{\infty} \frac{\left(\frac{\bar{\gamma}}{1+\bar{\gamma}}\right)^k}{k!(l+1)^{k+1}} \Gamma\left(k+1, \frac{(1+l)\bar{\gamma}\eta_T}{4}\right) \\ = \frac{1}{1+l(1+\bar{\gamma})} \exp\left(-\frac{\eta_T\bar{\gamma}(1+l(1+\bar{\gamma}))}{4(1+\bar{\gamma})}\right). \end{aligned} \quad (36)$$

The validity of (34) can be proved by first making the change of variables $z = (\bar{\gamma}/(1+\bar{\gamma}))$ on both sides of the equation.

Then, writing the Taylor series of the left of (34) in terms of z , the equality is readily obtained and hence, the proof is complete.

To prove (35), we first rewrite it as

$$\sum_{k=0}^{\infty} z^k \sum_{n=0}^k \frac{\left(\frac{z\eta_T}{1-z}\right)^n}{n!} = \frac{1}{1-z} \sum_{k=0}^{\infty} z^k \frac{\left(\frac{z\eta_T}{1-z}\right)^k}{k!} \quad (37)$$

where the change of variables $z = (\bar{\gamma}/(1+\bar{\gamma}))$ has been made. Next, substituting $1/1-z$ by its Taylor series, the right of (37) can be written as

$$\sum_{k=0}^{\infty} z^k \sum_{k=0}^{\infty} z^k \frac{\left(\frac{z\eta_T}{1-z}\right)^k}{k!}. \quad (38)$$

Now using [5, eq. (0.316)], the product of the two infinite sums in (38) can be shown to be equal to the left of (37) using routine algebra, and hence, the proof is complete.

To prove (36), we first rewrite it, after some mathematical manipulations, as

$$\begin{aligned} \exp\left(-\frac{(l+1)\eta_T\bar{\gamma}}{4}\right) \sum_{k=0}^{\infty} \frac{\left(\frac{\bar{\gamma}}{1+\bar{\gamma}}\right)^k}{(l+1)^{k+1}} \sum_{n=0}^k \frac{((1+l)\eta_T\bar{\gamma})^n}{4^n n!} \\ = \frac{\bar{\gamma}+1}{1+l(1+\bar{\gamma})} \exp\left(-\frac{\eta_T\bar{\gamma}(1+l(1+\bar{\gamma}))}{4(1+\bar{\gamma})}\right) \end{aligned} \quad (39)$$

where we have replaced the incomplete Gamma function by its series expansion, using [5, eq. (8.352.2)]. Next, combining the exponential terms and using (34), we obtain

$$\begin{aligned} \sum_{k=0}^{\infty} \frac{\left(\frac{\bar{\gamma}}{1+\bar{\gamma}}\right)^k}{(l+1)^{k+1}} \sum_{n=0}^k \frac{((1+l)\eta_T\bar{\gamma})^n}{4^n n!} \\ = \exp\left(\frac{\eta_T\bar{\gamma}^2}{4(1+\bar{\gamma})}\right) \sum_{k=0}^{\infty} \frac{\left(\frac{\bar{\gamma}}{1+\bar{\gamma}}\right)^k}{(l+1)^{k+1}}. \end{aligned} \quad (40)$$

Next, we replace the exponential term on the right of (40) by its Taylor series expanded in terms of x . Thus, we obtain

$$\begin{aligned} \sum_{k=0}^{\infty} \frac{\left(\frac{\bar{\gamma}}{1+\bar{\gamma}}\right)^k}{(l+1)^{k+1}} \sum_{n=0}^k \frac{((1+l)\eta_T\bar{\gamma})^n}{4^n n!} \\ = \sum_{k=0}^{\infty} \left(\frac{\bar{\gamma}}{\bar{\gamma}+1}\right)^k \frac{(\bar{\gamma}\eta_T)^k}{4^k k!} \sum_{k=0}^{\infty} \frac{\left(\frac{\bar{\gamma}}{1+\bar{\gamma}}\right)^k}{(l+1)^{k+1}}. \end{aligned} \quad (41)$$

Finally, using [5, eq. (0.316)] and some routine algebra, one can show that the product of the two infinite series on the right of (41) is equal to the left of (41), and hence, the proof is complete.

REFERENCES

- [1] M.-S. Alouini and M. K. Simon, "Postdetection switched combining—A simple diversity scheme with improved BER performance," *IEEE Trans. Commun.*, vol. 51, no. 9, pp. 1591–1602, Sep. 2003.
- [2] M. K. Simon and M.-S. Alouini, "Probability of error for noncoherent M -ary orthogonal FSK with postdetection switched combining," *IEEE Trans. Commun.*, vol. 51, no. 9, pp. 1456–1462, Sep. 2003.
- [3] J. G. Proakis, *Digital Communications*, 2nd ed. New York: McGraw-Hill, 1989.
- [4] M. K. Simon and M.-S. Alouini, *Digital Communication Over Fading Channels: A Unified Approach to Performance Analysis*. New York: Wiley, 2000.
- [5] I. S. Gradshteyn and I. M. Ryzhik, *Table of Integrals, Series and Products*, 6th ed. San Diego, CA: Academic, 2000.
- [6] A. Papoulis and S. U. Pillai, *Probability, Random Variables and Stochastic Processes*, 4th ed. New York: McGraw-Hill, 2002.



Sasan Haghani (S'01) received the B.Sc. (honors) degree in electrical engineering from Isfahan University of Technology, Isfahan, Iran, in 2000, and the M.Sc. degree in electrical engineering from the University of Alberta, Edmonton, AB, Canada, in 2002. Currently, he is working toward the Ph.D. degree in the iCORE Wireless Communications Laboratory, Department of Electrical and Computer Engineering, University of Alberta.

His current research interests include performance analysis of diversity-combining techniques and spread-spectrum systems.

Mr. Haghani is a recipient of postgraduate scholarships from the Alberta Ingenuity Fund and the Alberta Informatics Circle of Research Excellence (iCORE).



Norman C. Beaulieu (S'82–M'86–SM'89–F'99) received the B.A.Sc. (honors), M.A.Sc., and Ph.D. degrees in electrical engineering from the University of British Columbia, Vancouver, BC, Canada, in 1980, 1983, and 1986, respectively.

He was a Queen's National Scholar Assistant Professor with the Department of Electrical Engineering, Queen's University, Kingston, ON, Canada, from September 1986 to June 1988, an Associate Professor from July 1988 to June 1993, and a Professor from July 1993 to August 2000. In

September 2000, he became the iCORE Research Chair in Broadband Wireless Communications at the University of Alberta, Edmonton, AB, Canada, and in January 2001, the Canada Research Chair in Broadband Wireless Communications. His current research interests include broadband digital communications systems, fading channel modeling and simulation, interference prediction and cancellation, decision-feedback equalization, and space-time coding.

Dr. Beaulieu is a Member of the IEEE Communication Theory Committee and served as its Representative to the Technical Program Committee of the 1991 International Conference on Communications and as Co-Representative to the Technical Program Committee of the 1993 International Conference on Communications and the 1996 International Conference on Communications. He was General Chair of the Sixth Communication Theory Mini-Conference in association with GLOBECOM 97 and Co-Chair of the Canadian Workshop on Information Theory 1999. He has been an Editor for Wireless Communication Theory of the IEEE TRANSACTIONS ON COMMUNICATIONS since January 1992, and was Editor-in-Chief from January 2000 to December 2003. He served as an Associate Editor for Wireless Communication Theory of the *IEEE Communications Letters* from November 1996 to August 2003. He has also served on the Editorial Board of the *Proceedings of the IEEE* since November 2000. He received the Natural Science and Engineering Research Council of Canada (NSERC) E. W. R. Steacie Memorial Fellowship in 1999. He was awarded the University of British Columbia Special University Prize in Applied Science in 1980 as the highest standing graduate in the faculty of Applied Science. He is a Fellow of The Royal Society of Canada.